

Improving mechanical performance of soil-bentonite by slag cement addition

Amélioration des performances mécaniques du sol-bentonite par ajout de ciment de laitier

J. Chen*, Y. Masaki, A. Takai, T. Kato, T. Katsumi

Graduate School of Global Environmental Studies, Kyoto University, Japan

**chen.ji.68s@st.kyoto-u.ac.jp*

ABSTRACT: Soil bentonite (SB) mixtures generally presents inadequate mechanical properties compared to other cutoff wall materials. Since both deformability and a certain level of strength properties need to be achieved for static loads or in situations of dynamic loads, the cement amendment is adopted to improve the engineering performance and ensuring the long-term effectiveness of SB cutoff walls. This study investigated the strength properties and deformation characteristics of soil-bentonite mixtures amended with slag cement using Consolidated-Undrained (CU) triaxial tests. The contents of slag cement powder considered were 25, 50, and 75 kg/m³. The test results indicate that the undrained shear strength, residual shear strength and effective strength parameters are significantly influenced by the integration of cementation and consolidation. As compared in different cement addition, the 25 kg/m³ cement amended specimens shows strain-hardening behaviours, 42.7 to 65.1 kPa undrained shear strength in ductile failure mode with no discernible cracks, which signifying plastic deformation with high deformability under triaxial loading. This implies that, although the contents of the slag cement were not so high, such as 25 kg/m³, the amended soil-bentonite performed high strength and deformability.

RÉSUMÉ: Les mélanges de bentonite du sol (SB) présentent généralement des propriétés mécaniques insuffisantes par rapport aux autres matériaux de mur de séparation. Étant donné que la déformabilité et un certain niveau de propriétés de résistance doivent être atteints pour des charges statiques ou dans des situations de charges dynamiques, l'amendement au ciment est adopté pour améliorer les performances techniques et assurer l'efficacité à long terme des murs de séparation SB. Cette étude a examiné les propriétés de résistance et les caractéristiques de déformation de mélanges sol-bentonite amendés avec du ciment de laitier à l'aide d'essais triaxiaux consolidés-non drainés (CU). Les teneurs en poudre de ciment de laitier considérées étaient de 25, 50 et 75 kg/m³. Les résultats des tests indiquent que les paramètres de résistance au cisaillement non drainé, de résistance résiduelle au cisaillement et de résistance effective sont significativement influencés par l'intégration de la cimentation et de la consolidation. Comparés à différents ajouts de ciment, les échantillons modifiés au ciment de 25 kg/m³ présentent des comportements d'écrouissage, une résistance au cisaillement non drainé de 42,7 à 65,1 kPa en mode de rupture ductile sans fissures perceptibles, ce qui signifie une déformation plastique avec une déformabilité élevée sous chargement triaxial. Cela implique que, même si la teneur en ciment de laitier n'était pas si élevée, par exemple 25 kg/m³, le sol-bentonite amendé présentait une résistance et une déformabilité élevées.

Keywords: Soil-bentonite; slag cement amendment; consolidated-undrained triaxial test; mechanical performance.

1 INTRODUCTION

Soil-bentonite (SB) is widely applied in vertical cutoff walls for preventing the migration of contaminants to the aquifer, owing to extremely low hydraulic conductivity and high deformability (Takai, A. et al., 2016). However, SB exhibits relatively low shear strength, and the effectiveness will be influenced in situations of high hydraulic or seismic loads.

Cementitious additives are often utilized to enhance certain mechanical properties, such as internal friction angle, cohesion coefficient and unconfined compressive strength, of soft soils (Luis, A.L. et al., 2019). The slag cement, as one type of eco-friendly

material in cementitious additives, are often applied to improve the engineering properties and ensuring the long-term effectiveness of soft soils. In the application of vertical cutoff walls, it is worthy to investigate the enhanced mechanical performance and the variations in deformability in instances of relatively low content ratio of slag cement. Previous studies evaluated the compressive strength properties coupled with hydraulic performance of soil-cement-bentonite, but the deformation mode as the effect of cement amount was not studied (Ata, A.A., et al, 2015; Huang, X., et al., 2021).

In this paper, a series of Consolidated-Undrained (CU) triaxial tests on soil-bentonite (SB) and soil-bentonite with slag cement (SB-C) was conducted to investigate the variations in residual shear strength properties and effective strength parameters. Moreover, Young's modulus E_0 and secant modulus E_{50} , combining with three typical failure modes were summarised to further investigate the deformation modes and classify the capacities of SB and SB-C to simultaneously maintain both comprehensive shear strength and high deformability.

2 MATERIALS AND METHODS

2.1 Materials

Decomposed granite soil, which is widely distributed in Japan, was selected as the host soil. The bentonite used in this paper was sodium bentonite provided from Kunimine Industries Co., Ltd., Japan. For the cement amendment, the Portland Blast-Furnace Slag Cement was taken as the cement additive. The dry density of the decomposed granite soil, sodium bentonite and slag cement are 2.73, 2.60 and 3.04 g/cm³, respectively.

2.2 Methods

Before the triaxial test, cylindrical specimens with a height of 100 mm and a diameter of 50 mm were prepared and cured for 7 D. The summary of test scheme has been presented in Table 1.

Table 1. Summary of test scheme.

	Bentonite slurry (L/m ³)	Bentonite powder (kg/m ³)	Slag cement (kg/m ³)	Effective confining pressure (kPa)
C0			0	
C25	350	97.5	25	40, 80,
C50			50	160
C75			75	

The specimen mixing process of SB-C mixtures can be divided into four steps. Firstly, the bentonite slurry (5% bentonite by weight) was prepared 24 h ahead of time for sufficient hydration. Then, the dry decomposed granite soil was mixed with distilled water and bentonite slurry for 5 mins. The third step was adding the bentonite powder in two batches and mixing for 5 mins respectively. Finally, the slag cement powder was added and mixed for 10 mins. To ensure the homogeneity, the specimens were prepared with the target dry density of 1.30 g/cm³. After the mixing process, the mixtures were poured into plastic cylinder with vibration to eliminate air voids and

bubbles in the specimens. Summary of test scheme The specimens were then sealed immediately with plastic wrap and aluminum foil to minimize possible moisture change and cured at 20 °C for 7 days.

To evaluate the mechanical performance of SB and SB-C specimens, a series of consolidated-undrained (CU) triaxial test as per ASTM D4767-11 (ASTM International, 2020) were conducted. The schematic of the triaxial test apparatus is shown in Figure 1.

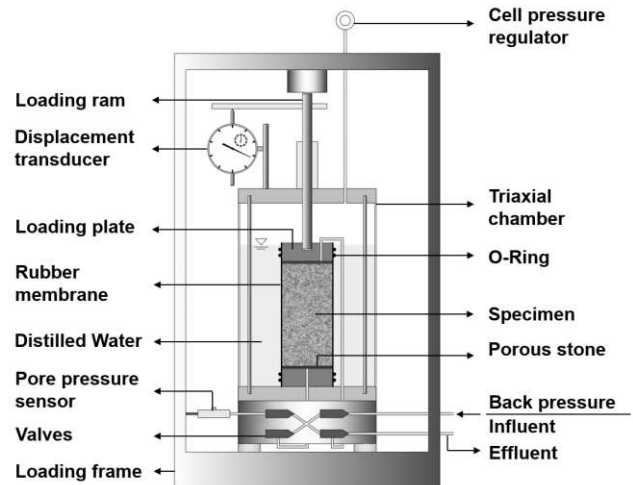


Figure 1. Schematic view of triaxial test apparatus.

For C0 specimens, after the third step of specimen mixing process, the soil-bentonite mixture was poured into a specially manufactured metal cylinder and installed in the triaxial chamber for saturation process. After 7 days curing, the C25/50/75 specimen was disassembled from the plastic cylinder and installed on the apparatus. In CU tests, specimens were saturated under a confining pressure of 10 kPa (i.e., a difference of 10 kPa between cell pressure and back pressure) until the B value is higher than 0.95. The specimens were then consolidated under different isotropic effective confining pressures (i.e., $\sigma_3 = q$ 40, 80 and 160 kPa) and sheared at an axial strain rate of 0.05 mm/min until reaching approximately 15% axial strain.

3 RESULTS AND DISCUSSION

3.1 Undrained shear strength properties

The results of the undrained shear strength (S_u) and failure axial strain obtained from the triaxial CU test as a function of cement addition under different effective confining pressure are presented in Table 2, where the value of S_u is equal to one half the deviator stress at failure. As according to the ASTM D4767-11 (ASTM International, 2020), the failure of specimen is corresponding to the maximum deviator stress (q_{max}) or deviator stress at 15% axial strain, whichever is the

first obtained during the test. The deviator stress (q) is determined using equation (1),

$$q = \sigma_1' - \sigma_3' \quad (1)$$

where σ_1' is the effective major stress and σ_3' is the effective minor principal stress.

Table 2. Undrained shear strength and failure axial strain.

	40 kPa		80 kPa		160 kPa	
	S_u (kPa)	ϵ_{peak} (%)	S_u (kPa)	ϵ_{peak} (%)	S_u (kPa)	ϵ_{peak} (%)
C0	10.5	15.0	17.5	15.0	30.4	15.0
C25	42.7	15.0	43.2	15.0	65.1	15.0
C50	94.1	13.1	89.6	11.7	117.6	12.6
C75	142.0	7.9	153.9	6.3	190.8	7.4

In Table 2, it can be seen that the value of S_u increases as the cement addition augments with almost double increment, which suggests the effect of cementation during curing process. The S_u value of C0 presents over half percent increasing from 10.5 kPa to 17.5 kPa under 40 and 80 kPa effective confining pressure, respectively. As the effective confining pressure rising from 40 kPa to 80 kPa, the value of S_u increases slightly in cement amended cases except for C50 with 4.5 kPa decrease. On the contrary, the S_u value of all the cases pronounce ascending trend when the effective confining pressure doubled from 80 kPa to 160 kPa.

It is indicated that, influenced by cementitious bonding, lower effective confining pressure exerts a reduced impact on the value of S_u . Moreover, all of the C0 and C25 specimens were sheared to S_u at the failure axial strain ϵ_{peak} of 15%. For C50, the ϵ_{peak} values were varying from 11.7% to 13.1%, while the ϵ_{peak} values of C75 were comparatively lower, from 6.3% to 7.4%. Figure 2 shows the variation of residual undrained shear strength (S_r) as the function of cement addition.

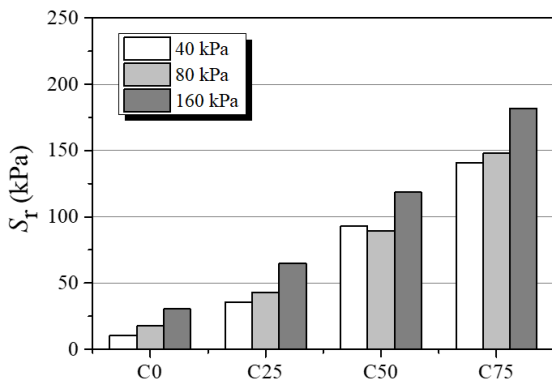


Figure 2. Residual undrained shear strength.

In Figure 2, the S_r is defined as half value of the deviator stress at 15% axial strain. It can be observed that the S_r increases with the increasing of confining pressure at a given cement amount except for the C50. Similar upward variation trend of S_r with the augment of cement addition can be found, as the variation trend of S_u in Table 2. Moreover, when comparing S_r with S_u , for C0 and C25, the S_r is about the same with S_u . For C50 and C75, the S_r is exceeding 90% on average the S_u , which points to high strength retention characteristics after failure.

3.2 Effective stress path and strength envelope

The results of the effective stress path and strength envelope are plotted in Figure 3. The mean effective stress p' is defined in equation (2):

$$p' = \frac{\sigma_1' + 2\sigma_3'}{3} \quad (2)$$

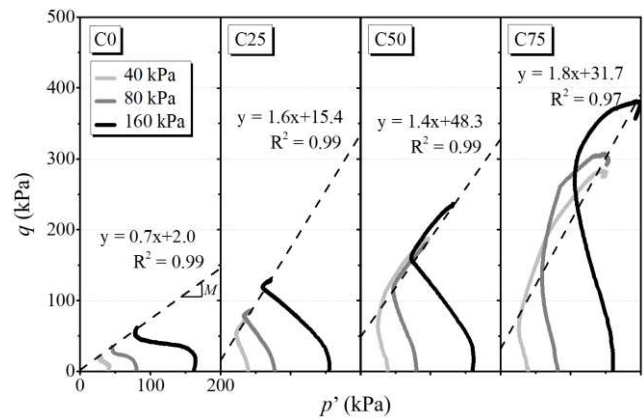


Figure 3. Effective stress path and strength envelope.

In Figure 3, the slope M of linear strength envelopes for SB (C0) and SB-C (C25, C50, C75) specimens were determined to estimate the effective strength parameters (c' and ϕ'). The relationship between the internal friction angle ϕ'_{peak} and the parameter M is expressed in equation (3) (Luis, A.L. et al., 2019):

$$M = \frac{6 \sin \phi'_{peak}}{3 - \sin \phi'_{peak}} \quad (3)$$

The effective cohesion (c') is determined using equation (4):

$$c' = \frac{c}{M} \quad (4)$$

where the c is the intercept with the q axis of the linear envelopes in Figure 3. The results of c' and ϕ' are summarized in Table 3.

Table 3. Effective strength parameters (c' /kPa, ϕ' /°).

C0		C25		C50		C75	
c'	ϕ'	c'	ϕ'	c'	ϕ'	c'	ϕ'
2.0	35.8	15.4	58.2	48.3	55.0	31.7	61.0

As shown in Figure 3, the gradients of these envelopes are similar in SB-C specimens as the ϕ' were ranging from 55.0° to 61.0°, which represents high shear strength. With low cement amount amended, the ϕ' of C25 is 58.2 kPa, higher than C50 and close to C75. The c' of C25 is 15.4 kPa, as 2.0 kPa of C0 with high deformability, and over 30 kPa for C50 and C75.

3.3 Elastic moduli and failure modes

To evaluate the deformation mode, the results of Young’s modulus E_0 and secant modulus E_{50} (defined at 50% of the peak strength) are illustrated in Figure 4.

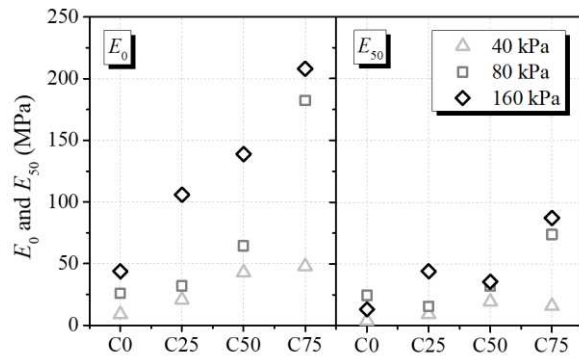


Figure 4. Young’s modulus E_0 and secant modulus E_{50} .

It is observed that the moduli (E_0 , E_{50}) increase with the augment of cement addition. When comparing the E_0 to E_{50} , it is evident that, the E_{50} is less than 50% of E_0 in all instances. It is noteworthy that this value does not align with that of typical elastic material, which tends to be significantly higher. It is also indicated the propensity for plastic deformation. Moreover, three typical failure modes are summarized in Figure 5.

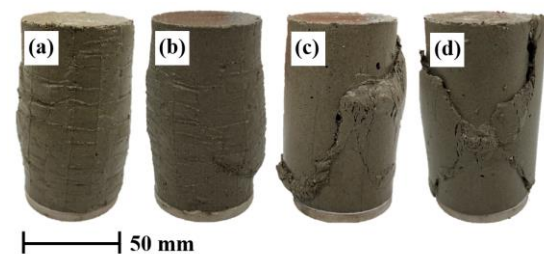


Figure 5. Typical failure modes

Figure 5 (a) was strain-hardening ductile failure in C0 and C25, while (b) presented planar failure in C50 under 40 kPa effective confining pressure. Figure 5 (c) and (d) are planar failure with larger failure angle in

C50 specimens, and split failure in all C75 specimens. This point can be explained by the hydration and pozzolanic reactions of cement, which result in the rigidity of specimens (Luis, A.L. et al., 2019).

4 CONCLUSIONS

In this paper, the slag cement amended SB-C specimens exhibit diverse mechanical performance.

The results indicate that C25 displays 42.7 to 65.1 kPa undrained shear strength with strain-hardening behaviours. No discernible cracks are observed at ductile failure, signifying plastic deformation with a high degree of deformability when subjected to triaxial loading. Comparing with C25, C0 presents the same failure mode with lower S_u , while planar failure and split failure can be observed in C50 and C75 with excessively higher S_u but lower deformability.

ACKNOWLEDGEMENTS

The authors are grateful for Mr. G. Araki (Raito Kogyo Co., Ltd.) and his colleagues for their great assistance on this research.

REFERENCES

ASTM D4767-11 (2020), Standard Test Method for Consolidated Undrained Triaxial Compression Test for Cohesive Soils, ASTM International, West Conshohocken, PA, the United States.

Ata, A.A., Salem, T.N., Elkhawas, N.M. (2015) Properties of soil–bentonite–cement bypass mixture for cutoff walls. *Construction and Building Materials*. 93: 950-956. <http://doi.org/10.1016/j.conbuildmat.2015.05.064>.

Huang, X., Li, J.S., Guo, M.Z., Xue, Q., Du, Y.J., Wan, Y., Liu, L., and Poon C.S. (2021) Using MgO activated slag and calcium bentonite slurry to produce a novel vertical barrier material: Performances and mechanisms. *Construction and Building Materials*. 291: 1-14. <http://doi.org/10.1016/j.conbuildmat.2021.123365>.

Luis, A.L. Deng, L. Shao, H.L. (2019) Triaxial behaviour and image analysis of Edmonton clay treated with cement and fly ash, *Construction and Building Materials*. 197: 208-219. <https://doi.org/10.1016/j.conbuildmat.2018.11.222>.

Takai, A., Inui, T., Katsumi T. (2016) Evaluating the hydraulic barrier performance of soil-bentonite cutoff walls using the piezocone penetration test, *Soils and Foundations*. 56(2): 277-290. <http://dx.doi.org/10.1016/j.sandf.2016.02.010>.

INTERNATIONAL SOCIETY FOR SOIL MECHANICS AND GEOTECHNICAL ENGINEERING



This paper was downloaded from the Online Library of the International Society for Soil Mechanics and Geotechnical Engineering (ISSMGE). The library is available here:

<https://www.issmge.org/publications/online-library>

This is an open-access database that archives thousands of papers published under the Auspices of the ISSMGE and maintained by the Innovation and Development Committee of ISSMGE.

The paper was published in the proceedings of the 18th European Conference on Soil Mechanics and Geotechnical Engineering and was edited by Nuno Guerra. The conference was held from August 26th to August 30th 2024 in Lisbon, Portugal.